

Measurement of electron temperature and density in an argon microdischarge by laser Thomson scattering

Sergey G. Belostotskiy,¹ Rahul Khandelwal,¹ Qiang Wang,¹ Vincent M. Donnelly,^{1,a)}
Demetre J. Economou,^{1,b)} and Nader Sadeghi²

¹*Plasma Processing Laboratory, Department of Chemical and Biomolecular Engineering,
University of Houston, Houston, Texas 77204-4004, USA*

²*Laboratoire de Spectrométrie Physique (UMR C5588), Université J. Fourier de Grenoble,
B P 87, F-38402 Saint-Martin d'Hères Cedex, France*

(Received 12 April 2008; accepted 12 May 2008; published online 6 June 2008)

Laser Thomson scattering in a novel, backscattered configuration was employed to measure the electron temperature (T_e) and electron density (n_e) in argon dc microdischarges, with an interelectrode gap of 600 μm . Measurements were performed at the center of the gap that corresponds to the positive column. For 50 mA microdischarge current and over the pressure range of 300–700 Torr, the plasma parameters were found to be $T_e=0.9 \pm 0.3$ eV and $n_e=(6 \pm 3) \times 10^{13} \text{ cm}^{-3}$, in reasonable agreement with the predictions of a mathematical model. © 2008 American Institute of Physics. [DOI: [10.1063/1.2939437](https://doi.org/10.1063/1.2939437)]

High pressure (hundreds of torr) nonequilibrium microdischarges have been the subject of extensive investigations.^{1–11} This is due to their unique properties that make such microdischarges applicable in plasma display panels, excimer radiation sources, sensors, chemical and biological microreactors, etc. To understand and optimize the operation of these devices, reliable diagnostics of microplasmas are highly desired. Plasma diagnostics of microdischarges are complicated because of their small size and the high operating pressure.

Laser Thomson scattering (LTS) allows direct and simultaneous measurement of both electron density and electron temperature. LTS has been widely used for diagnostics of high temperature, high density plasmas,^{12,13} as well as low pressure nonequilibrium discharges.^{14–20} LTS experiments in microdischarges are challenging because of the low signal and excessive stray light. Noguchi *et al.*⁷ used LTS to measure the electron temperature and density in a pulsed (10 kHz) dc argon microdischarge at a pressure of 50 Torr. Other groups have also performed LTS in different types of microdischarges.^{8,9} Kono *et al.*⁸ performed measurements in 2.45 GHz microwave microdischarges, sustained in a 100 μm gap at atmospheric pressures of air or a He/N₂ (5%) mixture. Hassaballa *et al.*⁹ studied a pulsed dc (20 kHz) microdischarge in Ne/Ar (10%) mixture at pressures of 100–300 Torr. No LTS measurements have been performed in argon microdischarges at higher pressures up to near atmospheric.

In this letter we report the results of direct measurements of electron temperature (T_e) and electron density (n_e) in argon dc microdischarges ($p=300$ –700 Torr) by using LTS.

The apparatus used for LTS was essentially identical to that described in Ref. 10 (see Fig. 1); therefore, only a brief description is given below. A dc glow discharge in Ar was ignited between two molybdenum electrodes (interelectrode gap $d=600 \mu\text{m}$, electrode surface area $5 \times 0.5 \text{ mm}^2$). The discharge current was set at $I=50$ mA, resulting in a voltage

between the electrodes in the range of 310–350 V (as pressure was varied). Higher currents resulted in glow-to-arc transition and damage of the electrodes.

The beam of a pulsed, frequency-doubled Nd:YLF (Neodymium: Yttrium Lithium Fluoride) laser (wavelength $\lambda=526.5$ nm, pulse frequency $f=3$ kHz, pulse duration $\tau \sim 100$ ns, and average power $P \sim 6$ W) was condensed by two lenses and guided into a specially designed periscope. The periscope (see expanded view in Fig. 1) consisted of a Brewster-angle window, a right-angle prism and a 3 mm diameter, 15 mm focal length lens that focused the beam into the microdischarge.

Backscattered light (confocal arrangement with scattering angle $\theta=180^\circ$) was collected by two lenses, spatially filtered by a 100 μm diameter pinhole, and focused on the 100 μm entrance slit of a triple grating spectrometer (TGS).^{15,19} Because of the small dimensions of the microplasma, stray laser light can be very strong. Moreover, the high operating pressure of the microdischarge results in high Rayleigh scattering intensity. The TGS provides very efficient spectral filtering of the scattered light at the laser (central) wavelength, while transmitting the light shifted with respect to the laser wavelength.

A 500 μm wide spatial filter was used in the TGS for the present measurements. The choice of spatial filter width is a compromise between blocked spectral range and laser wavelength suppression. In the case of rotational Raman spectroscopy (Ref. 10), a wider spatial filter (750 μm) could be used since the Raman peaks were sufficiently shifted from the laser wavelength. However, the spectral width of the Thomson signal ($\propto \sqrt{T_e}$) is relatively small due to the low electron temperatures (~ 3.5 nm for $T_e=1$ eV). A 500 μm wide filter was found to be the best compromise.

Light transmitted through the TGS was recorded by an intensified charge-coupled device (ICCD) camera in the gated mode, synchronized with the laser pulse. Spectra accumulated over 100 s (3×10^5 laser pulses) were recorded on a computer and processed by a LABVIEW program that implemented a nonlinear (Gaussian) least squares fitting routine. Data points in the spectral range blocked by the spatial filter

^{a)}Electronic mail: vmdonnelly@uh.edu.

^{b)}Electronic mail: economou@uh.edu.

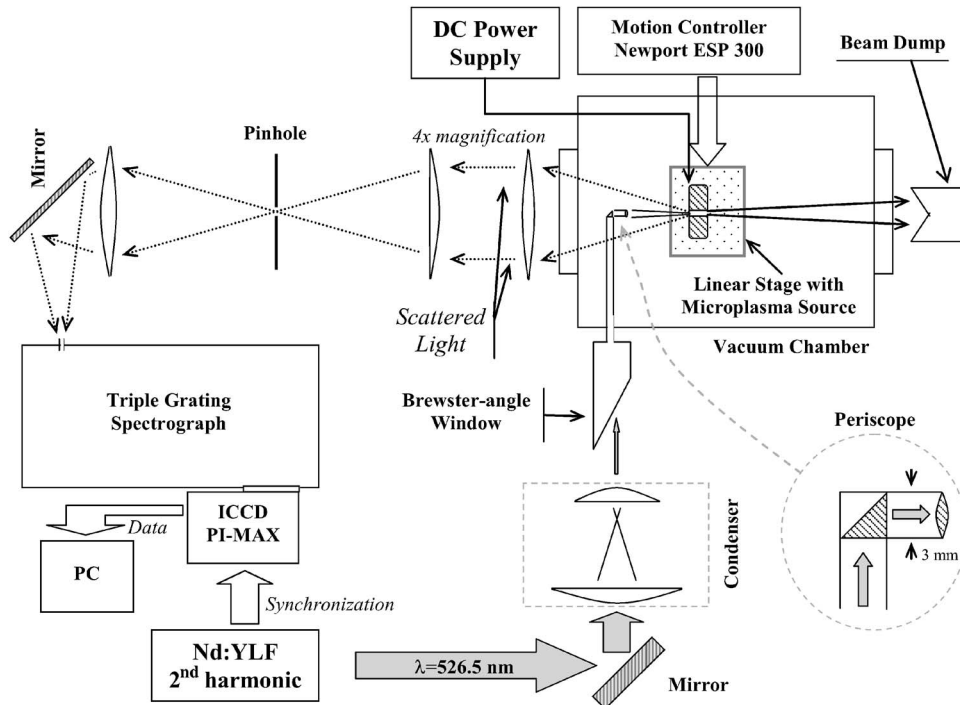


FIG. 1. Schematic diagram of the experimental setup (Ref. 10).

were not included in the fitting. Absolute calibration (required for extracting the absolute electron density n_e) was done using Raman scattering from nitrogen. Before and after a set of experiments, the chamber was evacuated and then filled with pure N₂. The calibration constant was found by fitting the Raman signal to a synthetic spectrum at room temperature (Ref. 10).

As pointed out in Ref. 10, the confocal geometry has certain advantages. First, it provides higher flexibility in microdischarge reactor design, since only one direction (the axis of the laser beam) has to remain unobstructed (typical light collection systems at 90° with respect to the laser beam require two optical axes). This aspect is especially important for microdevices. Also, the 180° scattering angle of the confocal geometry results in higher values of the differential cross section, and thus greater intensity. However, in the confocal geometry, the intensity of the stray laser radiation is much higher than in the 90° geometry. When the frequency shift of the signal is large enough, the required stray light reduction factor can be achieved by choosing a wide spatial filter in the TGS. On the other hand, when the frequency shift of the signal is small (e.g., Thomson scattering from low-temperature electrons) stray light rejection becomes a problem, hence it was difficult to carry out spatially resolved LTS measurements of T_e and n_e . The measurement point was chosen on the basis of minimizing stray laser light (approximately in the middle of the interelectrode gap).

To obtain a Thomson spectrum (Fig. 2) three consecutive signal accumulations were performed: scattered laser light with the plasma on, scattered laser light with the plasma off, and plasma emission (with laser off). The Thomson spectrum was found by subtracting the two latter spectra from the first one. Despite the presence of noise, the Gaussian fit was reasonably good (see Fig. 2).

Due to the rather long duration of the laser pulse (~100 ns), gating the ICCD did not provide sufficient suppression of the background plasma emission. The problem of background plasma emission also precluded the use of photo-

ton counting to improve the signal-to-noise ratio (the ICCD noise was relatively small compared to plasma emission). These problems were compensated by signal averaging over a very large number (3×10^5) of laser pulses. The high repetition rate allowed this data set to be collected in ~100 s.

The electron temperature can be extracted from the width of the Gaussian fit,^{14,15,20}

$$T_e = \frac{m_e c^2}{32 \ln 2} \left(\frac{\Delta\lambda_{1/2}}{\lambda_{\text{laser}}} \right)^2, \quad (1)$$

where m_e is the electron mass, c is the speed of light, λ_{laser} is the laser wavelength, and $\Delta\lambda_{1/2}$ is the full width at half maximum of the Gaussian function (T_e is in units of energy).

To obtain the absolute value of the electron density, a calibration was done by recording the rotational Raman

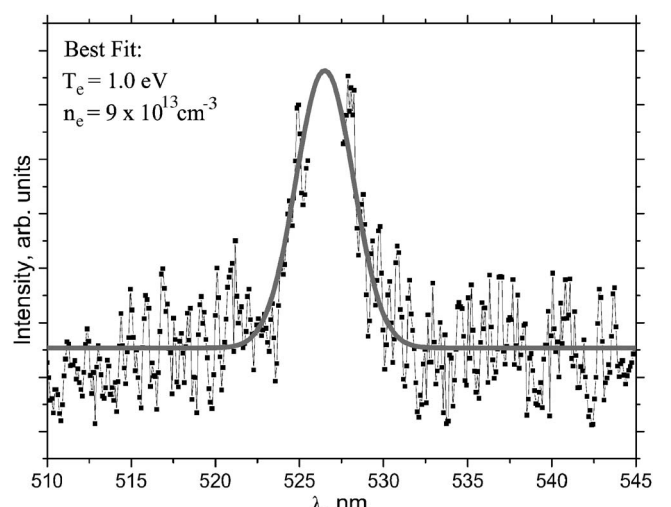


FIG. 2. An example of net (background subtracted) Thomson spectrum. The gray line is the best fit resulting in $T_e = 1.0$ eV and $n_e = 9 \times 10^{13}$ cm⁻³.

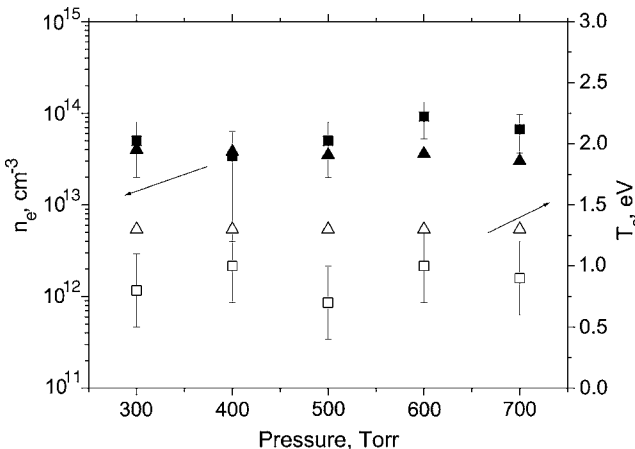


FIG. 3. Measured electron temperatures (open squares) and electron densities (solid squares) in a dc microdischarge at different argon pressures ($I=50$ mA). The corresponding electron temperatures (open triangles) and densities (solid triangles) predicted by a mathematical model are also indicated.

spectrum of N_2 at room temperature and specified pressure (600 Torr). Having determined the calibration factor, the electron density was found from,^{14,20}

$$n_e = CA \frac{2\lambda_{\text{laser}}}{r_e^2} \sqrt{\frac{2\pi T_e}{m_e c^2}}, \quad (2)$$

where C is the calibration factor, A is the pre-exponential factor of the Gaussian function ($f(\lambda) = A \exp\{-4 \ln(2) \cdot [(\lambda - \lambda_{\text{laser}})/\Delta\lambda_{1/2}]^2\}$), and $r_e = e^2/m_e c^2 = 2.818 \times 10^{-13}$ cm is the classical electron radius.

Measurements were done for a set of Ar pressures ($p=300\text{--}700$ Torr) with a discharge current of 50 mA (higher currents were not used due to arcing, while lower currents resulted in accordingly lower Thomson signals). The results are shown in Fig. 3. The electron temperature is quite low ($\sim 0.9 \pm 0.3$ eV), while the electron density is relatively high [$\sim (6 \pm 3) \times 10^{13}$ cm^{-3}]. There is essentially no pressure dependence within the uncertainty of the measurements.

The values of n_e and T_e shown in Fig. 3 are quite typical for this kind of microdischarge^{7,21} and are consistent with the predictions of a one-dimensional mathematical model, described in Ref. 21. The model employed the drift-diffusion approximation and included electrons (e), argon atomic ions Ar^+ , argon molecular ions Ar_2^+ , argon ground state atoms $\text{Ar}(^1\text{S}_0)$, two metastable states, $\text{Ar}(^3\text{P}_2)$ (or s_5 in Paschen notation) and $\text{Ar}(^3\text{P}_0)$ (or s_3 in Paschen notation), the resonant state $\text{Ar}(^3\text{P}_1)$ (or s_4), and excited dimmer molecules Ar_2^* . The model was analogous to the helium discharge studied in Ref. 22.

Figure 3 shows that the calculated electron temperatures are higher than the measured values. This discrepancy suggests that the positive column may be influenced by a beam of high energy electrons emanating from the cathode sheath, which creates a nonlocal ionization source, allowing for a

lower bulk electron temperature. Beam electrons were not treated in the fluid model which then predicts a higher electron temperature in the positive column.

In summary, LTS was employed to measure the electron temperature (T_e) and electron density (n_e) in argon dc microdischarges (interelectrode gap $d=600$ μm). A backscattering confocal optical system was developed for collecting the scattered light. Stray laser light and Raleigh scattering were blocked using a triple grating monochromator and spatial filters. Nitrogen Raman scattering was used to calibrate the scattered light intensity and extract the absolute electron density. Measurements were performed at the center of the gap that corresponds to the positive column. For the pressure range ($p=300\text{--}700$ Torr) and a discharge current of $I=50$ mA, the plasma parameters were found to be $T_e=0.9 \pm 0.3$ eV and $n_e=(6 \pm 3) \times 10^{13}$ cm^{-3} , almost independent of pressure. These values were in reasonable agreement with the predictions of a mathematical model.

The authors thank the Department of Energy (Grant No. DE-FG02-03ER54713) for funding this work and Professor A. Kono of Nagoya University for help with the design of TGS.

- ¹K. H. Becker, K. H. Schoenbach, and J. G. Eden, *J. Phys. D: Appl. Phys.* **39**, R55 (2006).
- ²M. Kushner, *J. Phys. D: Appl. Phys.* **38**, 1633 (2005).
- ³U. Kogelschatz, *Plasma Phys. Controlled Fusion* **46**, B63 (2004).
- ⁴J. P. Boef, *J. Phys. D: Appl. Phys.* **36**, R53 (2003).
- ⁵K. Tachibana, S. Kawai, H. Asai, N. Kikuchi, and S. Sakamoto, *J. Phys. D: Appl. Phys.* **38**, 1739 (2005).
- ⁶Q. Wang, I. Koleva, V. M. Donnelly, and D. J. Economou, *J. Phys. D: Appl. Phys.* **38**, 1690 (2005).
- ⁷Y. Noguchi, A. Matsuoka, M. D. Bowden, K. Uchino, and K. Muraoka, *Jpn. J. Appl. Phys., Part 1* **40**, 326 (2001).
- ⁸A. Kono and K. Iwamoto, *Jpn. J. Appl. Phys., Part 2* **43**, L1010 (2004).
- ⁹S. Hassaballa, M. Yakushiji, Y.-K. Kim, K. Tomita, K. Uchino, and K. Muraoka, *IEEE Trans. Plasma Sci.* **32**, 127 (2004).
- ¹⁰S. G. Belostotskiy, Q. Wang, V. M. Donnelly, D. J. Economou, and N. Sadeghi, *Appl. Phys. Lett.* **89**, 251503 (2006).
- ¹¹S. G. Belostotskiy, V. M. Donnelly, and D. J. Economou, *Plasma Sources Sci. Technol.* (unpublished).
- ¹²D. E. Evans and J. Katzenstein, *Rep. Prog. Phys.* **32**, 207 (1969).
- ¹³N. J. Peacock, D. C. Robinson, M. J. Forrest, P. D. Wilcock, and V. V. Sannikov, *Nature (London)* **224**, 488 (1969).
- ¹⁴M. J. van de Sande and J. J. A. M. van der Mullen, *J. Phys. D: Appl. Phys.* **35**, 1381 (2002).
- ¹⁵M. J. van de Sande, "Laser Scattering on Low Temperature Plasmas," Ph.D. thesis, Eindhoven University of Technology, 2002.
- ¹⁶T. Hori, M. Bowden, K. Uchino, and K. Muraoka, *J. Vac. Sci. Technol. A* **14**, 144 (1996).
- ¹⁷M. D. Bowden, T. Okamoto, F. Kimura, H. Muta, K. Uchino, K. Muraoka, T. Sakoda, M. Maeda, Y. Manabe, M. Kitagawa, and T. Kimura, *J. Appl. Phys.* **73**, 2732 (1993).
- ¹⁸K. Muraoka, K. Uchino, and M. D. Bowden, *Plasma Phys. Controlled Fusion* **40**, 1221 (1998).
- ¹⁹A. Kono and K. Nakatani, *Rev. Sci. Instrum.* **71**, 2716 (2002).
- ²⁰J. M. De Regt, R. A. H. Engeln, F. P. J. De Groot, J. A. M. van der Mullen, and D. C. Schram, *Rev. Sci. Instrum.* **66**, 3228 (1995).
- ²¹Q. Wang, "Plasma Diagnostics and Modeling of Direct Current Microplasma Discharges at Atmospheric Pressure," Ph.D. thesis, University of Houston, USA, 2006.
- ²²Q. Wang, D. J. Economou, and V. M. Donnelly, *J. Appl. Phys.* **100**, 023301 (2006).